2007

Concentration Dependent Fluorescence Lifetime in Nanocrystalline Y2O3:Eu Phosphors

Harald Kaps

Mohammad Lutful Arefin
Sheridan College, mohammad.arefin@sheridancollege.ca

Ulrich Herr

Heiko Paul

Concentration Dependent Fluorescence Lifetime in Nanocrystalline Y_2O_3:Eu Phosphors

Harald Kaps [1,a], Mohammad Lutful Arefin [2,b], Ulrich Herr [3,c] and Heiko Paul [3,d]

[1] Osram GmbH, Industriestraße, Herbrechtingen 89542, Germany
[2] Fraunhofer ISC (ISC), Neunerplatz 2, Würzburg 97082, Germany
[3] Ulm University, Albert-Einstein-Allee 47, Ulm 89081, Germany

e-mail: [a] haraldkaps@gmx.de, [b] arefin@isc.fraunhofer.de, [c] ulrich.herr@uni-ulm.de,
[d] heiko.paul@uni-ulm.de

Keywords: Y_2O_3:Eu, nanocrystalline, phosphor, UV-fluorescence spectroscopy, lifetime, diffusion limited energy transfer, chemical vapour reaction.

Abstract. Nanocrystalline $(Y_{1-x}Eu_x)_2O_3$ powder was synthesized via a chemical vapour reaction. X-ray diffraction revealed the structure of cubic yttria with crystallite sizes of about 5 nm. The Eu-dopand concentrations x for the samples in the range from 0.003 up to 0.165 were determined by EDX-spectra. The luminescence of the nanopowders was investigated by continuous and time-resolved UV-fluorescence spectroscopy and compared to a microcrystalline Y_2O_3:Eu phosphor as a reference. The emission spectra show an increasing intensity for higher doping concentrations. However, compared to the microcrystalline material the yield was significantly lower. The lifetime of the $^5D_0 - {}^7F_J$ transition in the nanocrystalline Y_2O_3:Eu was found to be significantly longer than for the microcrystalline reference sample. For increasing Eu-content the lifetime in the nanocrystalline samples decreased continuously from 3.71 ms to a value of 1.20 ms for the highest doping concentration. The concentration dependent lifetime behaviour was interpreted by energy transfer between Eu ions and from Eu ions to impurities as a competing process to the radiative $^5D_0 - {}^7F_2$ transition.

Introduction

In common fluorescent lamps typically three different phosphors are used to convert UV radiation into red, green and blue light. Cubic Y_2O_3:Eu is the most important red emitting ingredient for conversion layers due to its sharp $^5D_0 - {}^7F_2$ emission line in the red (611 nm) and a quantum efficiency of nearly 100% [1]. It also has widespread use in various display applications such as CRT and projection tubes.

Nanocrystalline phosphors are promising materials for further improvement of the excellent performance of this cubic Y_2O_3:Eu [2]. It has been demonstrated that nanocrystalline phosphors can achieve conversion efficiencies comparable to coarse grained Y_2O_3:Eu material. Several synthesis methods for nanosized Y_2O_3:Eu have been reported such as self-burning and sol-gel-technique [3, 4]. Using chemical vapour reaction (CVR) Konrad et al. were able to prepare weakly agglomerated nanocrystalline cubic Y_2O_3:Eu with a particle size of 10 nm for the first time [5]. A blue shift of absorption and reflection compared to coarse grained material was observed while the emission spectra remained unaltered.

In this work nanocrystalline cubic Y_2O_3:Eu powders have been produced using a chemical vapour reaction (CVR) process. The nanomaterials were characterized by X-ray analysis and UV-fluorescence spectroscopy. The main focus was on the behaviour of the lifetime τ of nanocrystalline cubic Eu-doped yttria as a function of the Eu^{3+} concentration. The results were compared with those of a microcrystalline reference material of similar compositions.

Model: Diffusion Limited Energy Transfer

In luminescent materials interactions between different types of ions often take place and have to be taken into account when modelling the lifetime behavior of a phosphor. In the Dexter model [6] the transfer probability between a sensitizer and an activator ion is given by

$$P_{SA} = \frac{1}{\tau_s} \left(\frac{R_0}{R} \right)^s \tag{1}$$

where R is the distance between the two ions, R_0 is a critical transfer distance, $1/\tau_S$ is the decay rate of the sensitizer emission and $s=6$ in the case of dipole-dipole-interaction.

At macroscopic scale, assuming a statistical arrangement of sensitizer and activator sites, including energy transfer between sensitizer atoms, the universal description of the intensity decay is complex [7]. However, for longer times t it can be written as an exponential decay with a measured lifetime τ [8]

$$\Phi(t) = \exp\left(-\frac{t}{\tau_0} - \frac{t}{\tau_D} \right) = \exp\left(-\frac{t}{\tau} \right). \tag{2}$$

where τ_0 is the lifetime of a single ion without energy transfer and τ_D is the contribution of energy transfer.

In the case of diffusion limited energy transfer (i.e. the decay rate of excited sensitizers is in the range of the rate of energy diffusion between sensitizers and the energy transfer rate from sensitizers to activators) the decay rate $1/\tau_D$ due to diffusion is [9]

$$\frac{1}{\tau_D} = 4\pi k C_{SA}^{\frac{1}{4}} C_{SS}^{\frac{3}{4}} N_A N_S \tag{3}$$

where N_A and N_S are the concentrations of activators and sensitizers, respectively. C_{SA} is the sensitizer-activator transfer constant while C_{SS} stands for the sensitizer-sensitizer transfer constant. The factor k is approximately 2.52.

A special application of this model is a phosphor consisting of luminescent centres in a host lattice which also contains impurities and/or defects. In this case the luminescent centres have to be identified by the sensitizer ions of the model and the impurities or defects are represented by the activators. As shown in Fig. 1 there are several pathways of decay in such a phosphor:

1) Direct emission from the excited luminescent centre,

2) single or multiple energy transfer between luminescent centres and subsequent emission from another luminescent centre,

3) energy transfer between luminescent centres (optional) preceding the transfer of energy from a luminescent centre to an impurity or defect in the neighbourhood where nonradiative decay takes place.
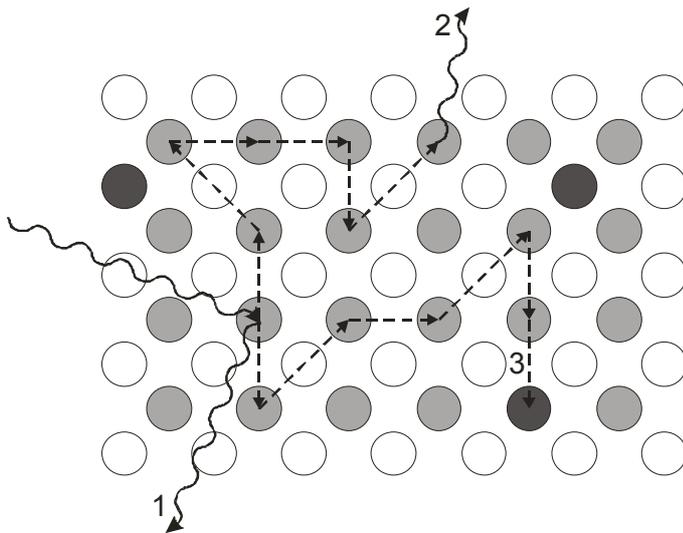
Figure 1. Energy transfer in a phosphor consisting of luminescent centers (grey) in a host lattice (white) with defects or impurities (dark): 1) direct emission, 2) emission after energy transfer between luminescent centers, 3) energy transfer to defect or impurity with nonradiative process

This nonradiative de-excitation mechanism is a process competing with the radiative transition within the luminescent center and causes the observed lifetime τ of the phosphor to decrease.

Experimental Details

The nanoparticles were synthesized by CVR [5, 10] using tetramethyl-heptandionato-yttrium $Y(C_{11}H_{19}O_2)_3$ and tetramethyl-heptandionato-europium $Eu(C_{11}H_{19}O_2)_3$ as metalorganic precursor materials. The precursors were heated in vapourizers totally immersed in temperature controlled oil baths. The Y-precursor was kept at a temperature of 433 K and the Eu-concentration was adjusted by selecting 403 K, 413 K, 423 K and 433 K as the Eu-precursor temperature. Argon as a carrier gas was passed through the vapourizers to transport the precursor vapour into the hot wall reactor which was at 1273 K and a pressure of 50 mbar. Oxygen was injected into the furnace as the reaction gas. Mass flow controllers were used to keep the flow rates at 200 ml/min and 800 ml/min for argon and oxygen, respectively. The synthesized powders were collected on a water-cooled cylinder at the end of the reaction chamber.

The Eu-concentration x of the $(Y_{1-x}Eu_x)_2O_3$ samples is derived from EDX-measurements. The phases and crystallite sizes by means were determined by X-ray diffraction using a Siemens D5005 diffractor. The Scherrer formula was used to calculate the crystallite sizes from the diffraction patterns. UV-fluorescence spectroscopy was carried out in a Jobin Yvon Fluorolog 3-22 spectrometer. Emission spectra were measured by exciting the phosphors at a wavelength of 254 nm thereby using the charge transfer transition to feed the Eu-emission. To determine the lifetime τ, time-resolved decay curves were recorded in the range from 0.05 ms to 10 ms with a step size of 0.05 ms and an integration time of 0.1 ms.

Results

The crystallite sizes of the as-prepared nanophosphors were in the range 5-7nm (see Table 1)

concentration x	crystallite size g [nm]	lifetime τ [ms]
0.003	6.5	3.71
0.024	5.2	3.08
0.052	5.4	2.40
0.165	5.5	1.20

Table 1. Compilation of crystallite sizes g and measured UV-fluorescence lifetimes τ of the 611 nm emission in the nanocrystalline $(Y_{1-x}Eu_x)_2O_3$ samples.

In Fig. 2 only the cubic phase of Y_2O_3 is identified by comparison of the diffraction pattern with JCPDS 43-1036 [11]. The sharp reflections in the pattern originate from the Si-wafer used as the sample holder for the nanopowders.
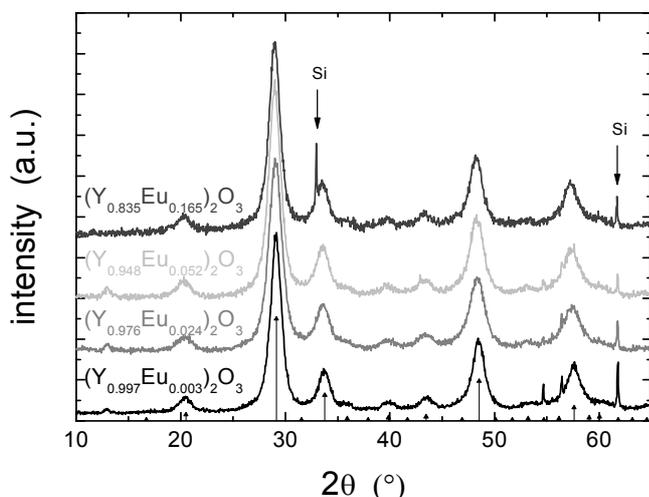

Figure *2*. X-ray diffraction patterns of the synthesized nanocrystalline Y_2O_3:Eu samples with $x=0.003$, $x=0.024$, $x=0.052$ and $x=0.165$ indicating the cubic structure of Y_2O_3 (JCPDS 43-1036 [11]) and a crystallite size between 5 nm and 7 nm for each concentration.

Fig. 3 depicts the emission spectra of the microcrystalline reference and the nanocrystalline CVR-samples. Most of the peaks can be identified with the C_2 lattice site, nevertheless, at 583 nm a peak of the C_{3i} site is also observed [12].
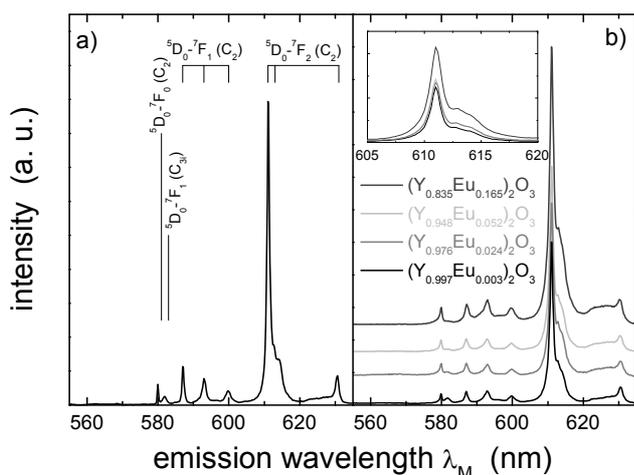

Figure 3. UV-fluorescence spectra of Y_2O_3:Eu at excitation wavelength $\lambda_X = 254$ nm: a) emission spectrum of the microcrystalline reference material ($x=0.035$), b) emission spectra of nanocrystalline CVR-samples for $x=0.003$, $x=0.024$, $x=0.052$ and $x=0.165$. The inset shows a blow-up of the region around the 611 nm line for intensity comparison.

In Fig. 3a the peaks of the reference sample are identified with the corresponding $^5D_0 - {}^7F_J$ transition of Eu. The peak positions in the nanomaterials, shown in Fig. 3b, are at the same positions as in the case of the microcrystalline sample, but the intensity is approximately one order of magnitude lower for similar Eu-concentrations.

The peak width of the nanocrystalline spectra is enhanced with respect to the microcrystalline reference. To compare the emission of the nanocrystalline samples, the inset in Fig. 3b shows the spectra only in the region of the 611 nm line. The intensity of the 611 nm line increases continuously with Eu-concentration. However, no strictly linear dependence is observed.

Fig. 4 shows decay curves for the $^5D_0 - {}^7F_2$ line at 611 nm for the different Eu doping concentrations of the nanocrystalline powders. The curves have been normalized to maximum intensity for better comparison of the decay behaviour. The lines drawn in the graph are monoexponential fits of the fluorescence data. With decreasing concentration of Eu in the Y_2O_3 matrix the measured lifetime τ of the decay rises from 1.20 ms to 3.71 ms (see Table 1).
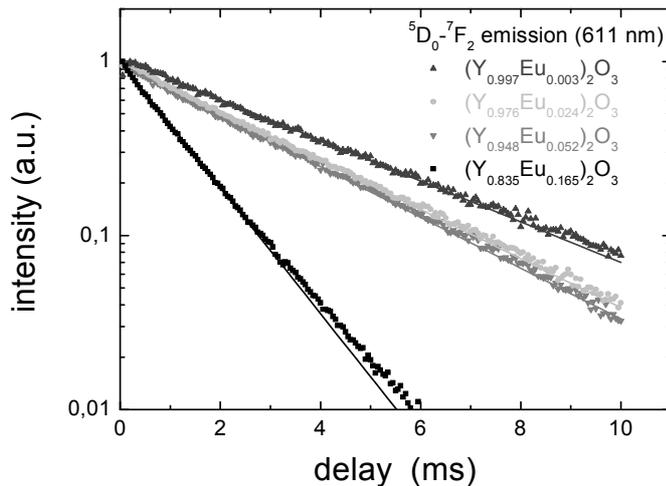
Figure 4. Luminescence decay curves of the $^5D_0 - {}^7F_2$ emission of nanocrystalline $(Y_{1-x}Eu_x)_2O_3$ for $x=0.003$, $x=0.024$, $x=0.052$ and $x=0.165$ at an excitation wavelength of 254 nm. The lines indicate single exponential fits of the measured data.

To investigate the concentration dependence in the microcrystalline case, coarse grained Y_2O_3:Eu powders at various compositions were produced in addition to the reference with $x=0.035$ by firing mixtures of Y_2O_3 and Eu_2O_3 at 1673 K. It was found that the concentration dependence is significantly smaller than in the nanocrystalline case: The measured lifetime τ reduces with increasing Eu-content from 1.10 ms down to 1.00 ms as shown in Table 2.

concentration x	lifetime τ [ms]
0.003	1.10
0.035	1.07
0.052	1.02
0.165	1.00

Table 2. Compilation of measured UV-fluorescence lifetimes τ of the 611 nm emission in the microcrystalline $(Y_{1-x}Eu_x)_2O_3$ samples.

Discussion

In Y_2O_3:Eu energy transfer can occur between the Eu-ions and from the Eu to impurities or defects. The model of diffusion limited energy transfer, as treated in the second section, predicts a decreased observed lifetime τ as a result of Eq. 2. This is caused by an additional decay rate $1/\tau_D$ proportional to the Eu-concentration according to Eq. 3. Fig. 5 shows the results of the lifetime τ measurements together with fits in accordance with Eq. 2 and 3 using τ_0 and the constant of proportionality (see Eq. 3) between $1/\tau_D$ and the Eu-concentration x (corresponding to N_S in Eq. 3) as the fitting parameters. The lifetime τ_0 obtained from the fits are $\tau_0 = 3.90$ ms for the CVR-samples and $\tau_0 = 1.09$ ms for the microcrystalline samples. The constant of proportionality between $1/\tau_D$ and the Eu-concentration x is larger in the nanoparticles (3.17 ms^{-1}) compared to the coarse grained material (0.58 ms^{-1}). According to the model, this can either be caused by modified transfer constants C_{SA} or C_{SS} or by a higher concentration of impurities N_A in the nanocrystalline material. If the impurity concentration N_A is associated with surfaces or interfaces then an increase of N_A in the nanophosphors appears highly probable due to the increased fraction of atoms at the particle surfaces of the nanophospors compared to the microcrystalline material.

The measured lifetime values τ of nano-Y_2O_3:Eu synthesized via CVR by Schmechel et al. [13] are also presented in Fig. 5. It is observed that they correspond well with the fit. It can be concluded that the data by Schmechel et al. can also be described by the energy transfer model.
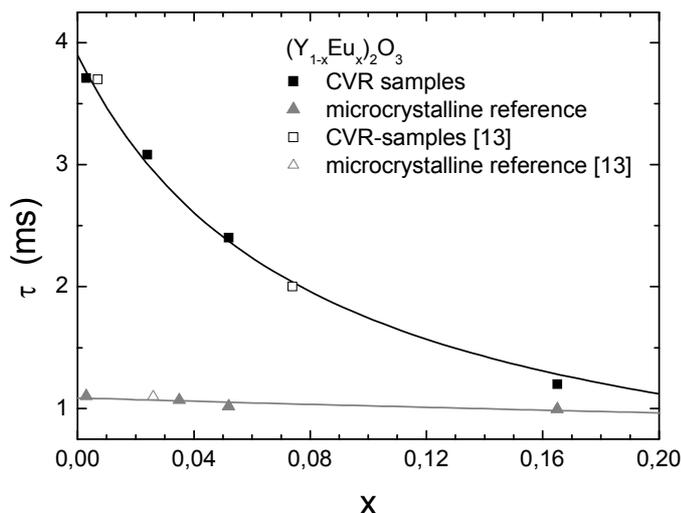
Figure 5. Measured lifetime τ of the 611 nm emission in Y_2O_3:Eu at various concentrations. The values in nanocrystalline Y_2O_3:Eu are enhanced compared to the ones in microcrystalline material - to an increasing degree at lower doping concentrations. The lines correspond to fits according to the model of diffusion limited energy transfer. The measured data of Schmechel et al. [13] represented by the outlined symbols also fit well into the concentration behavior.

In a nanocrystalline phosphor with a lower quantum efficiency than coarse grained material one would expect shorter lifetimes τ to be observed [13]. However, in the produced nanocrystalline Y_2O_3:Eu samples the emission intensity is lower than in the microcrystalline reference while the lifetime τ is longer. An enhancement of τ in the nanocrystalline material has also been found by Schmechel et al. [13]. However, the occurrence of longer lifetimes τ and lower intensities at the same time is not a contradiction since for the emission intensity, the absorbed fraction of the exciting radiation has to be taken into account. The higher reflectivity of nanocrystalline Y_2O_3:Eu in the charge transfer region observed by Konrad et al. [5] may therefore cause a strong reduction of the emission intensity in case of the nanocrystalline samples. The lifetime measurement, however, is only probing the radiative transition and is not affected by the low efficiency of absorption.

Summary

Nanocrystalline cubic Y_2O_3:Eu with a crystallite size of 5-7 nm was produced by CVR-synthesis with various Eu concentrations in the range of *x*=0.003 to *x*=0.165. UV-fluorescence spectroscopy shows lower intensities of the emission spectra in comparison to the coarse grained reference. The measured lifetimes τ of the Eu $^5D_0 - {}^7F_2$ decay are enhanced in the nanocrystalline material and show a strong dependence on the Eu-concentration with higher lifetimes at low Eu-concentrations. The variation of τ with doping concentration is less pronounced in the microcrystalline material. This behaviour has been described by the model of diffusion limited energy transfer between Eu-ions and from Eu-ions to impurities.

References

[1] G. Blasse and B.C. Grabmaier: Luminescent Materials (Springer Verlag, Berlin, 1994)
[2] U. Herr, H. Kaps and A. Konrad: Solid State Phenomena Vol. 94 (2003) p. 85
[3] M. Kottaisamy, D. Jeyakumar, R. Jagannathan and M. Mohan Rao: Mater. Res. Bull. Vol. 31 (1996) p. 1013
[4] Y. Tao, G. Zhao, X. Ju, X. Shao, W. Zhang and S. Xia: Mater. Lett. Vol. 28 (1996) p. 137
[5] A. Konrad, T. Fries, A. Gahn, F. Kummer, U. Herr, R. Tidecks and K. Samwer: J. Appl. Phys. Vol. 86 (1999) p. 3129
[6] D.L. Dexter: J. Chem. Phys. Vol 21 (1953) p. 836
[7] M. Yokota and O. Tanimoto: J. Phys. Soc. Jpn. Vol. 22 (1967) p. 779
[8] M.J. Weber: Phys Rev. B Vol. 4 (1971) p. 2932
[9] P.G. de Gennes: J. Phys. Chem. Solids Vol. 7 (1958) p. 345
[10] A. Konrad, T. Fries, A. Gahn, F. Kummer, U. Herr, R. Tiedecks and K. Samwer: Chem. Vap. Deposition Vol. 5 (1999) p. 207

[11] JCPDS Powder Diffraction File, Joint Commitee on Powder Diffraction Data (JCPDS International Centre for Diffraction Standards, Swarthmore)

[12] J. Heber, K.H. Hellwege, U. Köbler and H. Murmann: Z. Physik Vol. 237 (1970) p. 189

[13] R. Schmechel, M. Kennedy, H. von Seggern, H. Winkler, M. Kolbe, R.A. Fischer, L. Xaomao, A. Benker, M. Winterer and H. Hahn, J. Appl. Phys. Vol. 89 (2001) p. 1679